80	川原一郎, 森川実, 本田優, 北川直毅, 堤圭介, **永田泉** 造影MRIによるplaque imagingについての検討	造影MRIによるplaque imagingについての検討	The Mt. Fuji Workshop on CVD		Vol.24 :74-77 2006
81	**永田泉**	Microscopic carotid endarterectomy.	The 8th Korean and Japanese Friendship Conference on Surgery for Cerebral Stroke 8.5-6, 2006. 仙台		
82	**永田泉**	Microsurgical carotid endarterectomy.	The First Italian-Japanese Neurosurgical Workshop 10.15, 2006. 京都		
83	**永田泉**	Technical Aspects of Carotid Endarterectomy under Operative Microscope	2006 Conference of Asia Academic Neurosurgeons 11.10～12, 2006. 上海		
84	Yano S, **Kuroda S**, Shichinohe H, Seki T, Ohnishi T, Tamagami H, Hida K, Iwasaki Y	Bone Marrow Stromal Cell Transplantation Preserves Gammaaminobutyric Acid Receptor Function in the Injured Spinal Cord.	J Neurotrauma		23:1682-1692, 2006.
85	Ishikawa T, Kamiyama H, **Kuroda S**, Yasuda H, Nakayama N, Takizawa K:	Simultaneous superficial temporal artery to middle cerebral or anterior cerebral artery bypass with pan-synangiosis for Moyamoya disease covering	Neurol Med Chir (Tokyo)		46:462-468, 2006.

		both anterior and middle cerebral artery territories.			
86	Ito M, Kuroda S, Takano K, Maruichi K, Chiba Y, Morimoto Y, Iwasaki Y:	Motor cortex stimulation for post-stroke pain using neuronavigation and evoked potentials: report of 3 cases.	No Shinkei Geka		34:919-924, 2006.
87	Ishikawa T, Nakayama N, Yoshimoto T, Aoki T, Terasaka S, Nomura M, Takahashi A, **Kuroda S**, Iwasaki Y	How does spontaneous hemostasis occur in ruptured cerebral aneurysms? Preliminary investigation on 247 clipping surgeries.	Surg Neurol		66:269-275, 2006.
88	Niiya Y, Abumiya T, Shichinohe H, **Kuroda S**, Kikuchi S, Ieko M, Yamagishi S, Takeuchi M, Sato T, Iwasaki Y	Susceptibility of brain microvascular endothelial cells to advanced glycation end products-induced tissue factor upregulation is associated with intracellular reactive oxygen species.	Brain Res		1108:179-187, 2006.
89	Yamaguchi S, **Kuroda S**, Kobayashi H, Shichinohe H, Yano S, Hida K, Shinpo K, Kikuchi S, Iwasaki Y	The effects of neuronal induction on gene expression profile in bone marrow stromal cells (BMSC)--a preliminary study using microarray analysis.	Brain Res		1087:15-27, 2006.
90	Osanai T, **Kuroda S**, Ishikawa T, Kudo K, Terae S, Isobe M, Iwasaki Y	Repeated, reversible MR angiographic findings in pediatric moyamoya disease: case report.	No Shinkei Geka		34:403-407, 2006.
91	Shichinohe H, **Kuroda S**, Yano S, Ohnishi T, Tamagami H, Hida K, Iwasaki Y	Improved expression of gamma-aminobutyric acid receptor in mice with cerebral infarct and transplanted bone	J Nucl Med		47:486-491, 2006.

		marrow stromal cells: an autoradiographic and histologic analysis			
92	**Kuroda S**, Shiga T, Houkin K, Ishikawa T, Katoh C, Tamaki N, Iwasaki Y	Cerebral oxygen metabolism and neuronal integrity in patients with impaired vasoreactivity attributable to occlusive carotid artery disease.	Stroke		37:393-398, 2006.
93	Nanba R, **Kuroda S**, Tada M, Ishikawa T, Houkin K, Iwasaki Y	Clinical features of familial moyamoya disease.	Child Nerv Syst		22:258-262, 2006.
94	Kashiwazaki D, **Kuroda S**, Terasaka S, Iwasaki Y	Detection of hemodynamic transient ischemic attack during hemodialysis with near-infrared monitoring in a patient with internal carotid artery occlusion.	Surg Neurol		2006, in press.
95	鐙谷武雄、七戸秀夫、**黒田　敏**、石川達哉、岩崎喜信、小林祥泰	脳卒中データバンクを利用したくも膜下出血の解析−発症年齢、性差、予後における全国・地域別の検討−	脳卒中の外科]		34:49-53, 2006.
96	長内俊也、**黒田　敏**、石川達哉、工藤興亮、寺江聡、磯部正則、岩崎喜信	可逆的な動脈狭窄を繰り返した小児もやもや病の１例	脳外		34:403-407, 2006
97	**黒田　敏**	内頚動脈閉塞症にともなう血行力学的脳梗塞の発症予防に関する研究	厚生労働科学研究費補助金（循環器疾患等総合研究事業）平成 17 年度総括・分担研究報告書		Pp30-31, 2006.
98	山口　秀、**黒田　敏**、小	脳出血で発症した神経サル	脳外		34:839-842, 2006

	林浩之、丸一勝彦、久保田佳奈子、伊藤智雄、岩崎喜信	コイドーシスの一例			
99	**黒田　敏**	コイル塞栓術後の脳動脈瘤に対してクリッピング術を行なう際にはどのような点に注意すべきか？	片山容一、川又達朗（編）脳神経外科・専門医にきく最新の臨床		pp 25-31, 2006.
100	**黒田　敏**	脳血行再建術と脳循環・代謝	賓金清博（編）脳血行再建術の理論と実際	中外医学社	Pp 36-82, 2006.
101	伊東雅基、**黒田　敏**、高野和哉、丸一勝彦、千葉泰弘、森本裕二、岩崎喜信	中枢性疼痛に対する運動領野刺激療法–術中モニタリングによる工夫–	脳外	中外医学社	34:919-924, 2006.
102	**黒田　敏**、岩崎喜信	骨髄間質細胞を用いた脊髄損傷の再生は”Mission Impossible”か？	分子脳血管病		5: 436-442, 2006.
103	**黒田　敏**、寺坂俊介、石川達哉、牛越　聡、柏崎大奈、七戸秀夫、浅野剛、布村　充、鐙谷武雄、岩崎喜信	重症心・大動脈疾患を合併した無症候性内頚動脈狭窄症の治療方針と成績	脳卒中の外科		34:323-327, 2006.
104	寺坂俊介、岩崎喜信、**黒田　敏**、内田隆徳	ポリグリコール酸不織布フェルトとフィブリン糊による新しい硬膜閉鎖法–臨床応用 140 例の結果–	脳外		34:1109-1117, 2006
105	**黒田　敏**、岩崎喜信	家族性もやもや病。インターベンション時代の脳卒中学（改訂第２版）・下–超急	日本臨床		64:750-754, 2006

		性期から再発予防まで一			
106	**Kuroda S**, Ishikawa T, Nakayama N, Houkin K, Iwasaki Y	Moyamoya disease and pregnancy – a prospective study.]	International Stroke Conference 2007, February 7-9, 2007 (San Francisco)		
107	**Kuroda S**, Ishikawa T, Nakayama N, Houkin K, Iwasaki Y	Bypass surgery improves cerebral oxygen metabolism in pediatric, but not adult, moyamoya disease – a PET study.	Annual Meeting of American Association of Neurological Surgeons (AANS) 2007, April 23-27, 2006 (San Francisco)		
108	Ishikawa T, Kamiyama H, **Kuroda S**, Yasuda H, Nakayama N, Takizawa K	Simultaneous superficial temporal artery to middle cerebral or anterior cerebral artery bypass with pan-synangiosis for Moyamoya disease covering both anterior and middle cerebral artery territories.	Neurol Med Chir (Tokyo)		46(9):462-468, 2006.
109	Ito M, **Kuroda S**, Takano K, Maruichi K, Chiba Y, Morimoto Y, Iwasaki Y	Motor cortex stimulation for post-stroke pain using neuronavigation and evoked potentials: report of 3 cases	No Shinkei Geka		34:919-924, 2006.
110	Ishikawa T, Nakayama N, Yoshimoto T, Aoki T, Terasaka S, Nomura M, Takahashi A, **Kuroda S**, Iwasaki Y	How does spontaneous hemostasis occur in ruptured cerebral aneurysms? Preliminary investigation on 247 clipping surgeries.	Surg Neurol		66:269-275, 2006.
111	Niiya Y, Abumiya T, Shichinohe H, **Kuroda S,** Kikuchi S, Ieko M,	Susceptibility of brain microvascular endothelial cells to advanced glycation	Brain Res		1108:179-187, 2006.

	Yamagishi S, Takeuchi M, Sato T, Iwasaki Y	end products-induced tissue factor upregulation is associated with intracellular reactive oxygen species.			
112	Yamaguchi S, **Kuroda S**, Kobayashi H, Shichinohe H, Yano S, Hida K, Shinpo K, Kikuchi S, Iwasaki Y	The effects of neuronal induction on gene expression profile in bone marrow stromal cells (BMSC)--a preliminary study using microarray analysis.	Brain Res		1087:15-27, 2006.
113	Osanai T, **Kuroda S,** Ishikawa T, Kudo K, Terae S, Isobe M, Iwasaki Y	Repeated, reversible MR angiographic findings in pediatric moyamoya disease: case report.	No Shinkei Geka		34:403-407, 2006.
114	Shichinohe H, **Kuroda S**, Yano S, Ohnishi T, Tamagami H, Hida K, Iwasaki Y	Improved expression of gamma-aminobutyric acid receptor in mice with cerebral infarct and transplanted bone marrow stromal cells: an autoradiographic and histologic analysis.	J Nucl Med		47:486-491, 2006.
115	**Kuroda S**, Shiga T, Houkin K, Ishikawa T, Katoh C, Tamaki N, Iwasaki Y	Cerebral oxygen metabolism and neuronal integrity in patients with impaired vasoreactivity attributable to occlusive carotid artery disease.	Stroke		37:393-398, 2006.
116	Iihara K, Murao K, Sakai N, Yamada N, **Nagata I**, **Miyamoto S**	Outcome of carotid endarterectomy and stent insertion based on grading of carotid endarterectomy risk: a 7-year prospective study.	J Neurosurg		105:546-54, 2006.

117	**Kikuta KI**, Takagi Y, Fushimi Y, Ishizu K, Okada T, Hanakawa T, Miki Y, Fukuyama H, Nozaki K, **Hashimoto N.** .	"Target Bypass": A Method for Preoperative Targeting of a Recipient Artery in Superficial Temporal Artery-to-Middle Cerebral Artery Anastomoses.	Neurosurgery		59(4 Suppl 2):ONS320-ONS327
118	Takagi Y, **Kikuta K**, Sadamasa N, Nozaki K, **Hashimoto N** Caspase-3-dependent apoptosis in middle cerebral arteries in patients with moyamoya disease.	Caspase-3-dependent apoptosis in middle cerebral arteries in patients with moyamoya disease	Neurosurgery		59:894-900, 2006.
119	Ohta T, **Kikuta K**, Imamura H, Takagi Y, Nishimura M, Arakawa Y, **Hashimoto N**, Nozaki K	Administration of ex vivo-expanded bone marrow-derived endothelial progenitor cells attenuates focal cerebral ischemia-reperfusion injury in rats.	Neurosurgery		59:679-686, 2006.
120	Okada T, Mikuni N, Miki Y, **Kikuta K**, Urayama S, Hanakawa T, Fushimi Y,Yamamoto A, Kanagaki M, Fukuyama H, **Hashimoto N**, Togashi K	Corticospinal tract localization: integration of diffusion-tensor tractography at 3-T MR imaging with intraoperative white matter stimulation mapping--preliminary results.	Radiology		240:849-857, 2006.
121	Mineharu Y, Takenaka K, Yamakawa H, Inoue K, Ikeda H, **Kikuta KI**, Takagi Y, Nozaki K, **Hashimoto N**, **Koizumi A**	Inheritance pattern of familial moyamoya disease: autosomal dominant mode and genomic imprinting.	J Neurol Neurosurg Psychiatry		77:1025-1029, 2006.

122	Fushimi Y, Miki Y, Takahashi JA, **Kikuta K, Hashimoto N**, Hanakawa T, Fukuyama H, Togashi K	MR imaging of Liliequist's membrane	Radiat Med		24:85-90, 2006.
123	**Kikuta K**, Takagi Y, Arakawa Y, Miyamoto S, **Hashimoto N**:	Absence epilepsy associated with moyamoya disease. Case report.	J Neurosurg		104(4 Suppl):265-268, 2006.
124	Nozaki K, **Hashimoto N**, **Kikuta K,** Takagi Y, Kikuchi H:	Surgical applications to arteriovenous malformations involving the brainstem	Neurosurgery		58(4 Suppl 2): ONS-270-278, 2006.
125	Takagi Y, **Kikuta K**, Sadamasa N, Nozaki K, **Hashimoto N**	Proliferative activity through extracellular signal-regulated kinase of smooth muscle cells in vascular walls of cerebral arteriovenous malformations.	Neurosurgery		58:740-748, 2006.
126	Fushimi Y, Miki Y, **Kikuta K,** Okada T, Kanagaki M, Yamamoto A, Nozaki K, **Hashimoto N**, Hanakawa T, Fukuyama H, Togashi K	Comparison of 3.0- and 1.5-T three-dimensional time-of-flight MR angiography in moyamoya disease: preliminary experience.	Radiology		239:232-237, 2006.
127	**Kikuta K**, Takagi Y, Nozaki K, Hanakawa T, Okada T, Miki Y, Fushimi Y, Fukuyama H, **Hashimoto N**	Early experience with 3-T magnetic resonance tractography in the surgery of cerebral arteriovenous malformations in and around the visual pathway.	Neurosurgery		58:331-337, 2006.
128	Morizane A, Takahashi J, Shinoyama M, Ideguchi	Generation of graftable dopaminergic neuron	J Neurosci Res.		83:1015-1027, 2006.

	M, Takagi Y, Fukuda H, Koyanagi M, Sasai Y, **Hashimoto N**	progenitors from mouse ES cells by a combination of coculture and neurosphere methods.			
129	Moriwaki T, Takagi Y, Sadamasa N, Aoki T, Nozaki K, **Hashimoto N**	Impaired progression of cerebral aneurysms in interleukin-1beta-deficient mice.	Stroke		37::900-905, 2006.
130	Hayashi J, Takagi Y, Fukuda H, Imazato T, Nishimura M, Fujimoto M, Takahashi J, **Hashimoto N**, Nozaki K	Primate embryonic stem cell-derived neuronal progenitors transplanted into ischemic brain.	J Cereb Blood Flow Metab		26(7):906-914, 2006.
131	**菊田健一郎、橋本信夫**	脳卒中の外科治療の実態と新しい展開	インターベンション時代の脳卒中学（改訂第２版）・下−超急性期から再発予防まで−日本臨床		64:pp482-488, 2006
132	**Kikuta K**;	Surgical experiences for moyamoya disease by using 3T magnetic resonance imaging.	Abstract of the 3rd Europian-Japanese Joint Conference for Stroke Surgery, 2006.		
133	**Kikuta K, Hashimoto N**	Surgical experiences for brain arteriovenous malformations by using 3T magnetic resonance tractography.	Abstract of the 3rd Europian-Japanese Joint Conference for Stroke Surgery,		

doi:10.1093/brain/awl207 Brain (2006), 129, 2734–2745

Neuroprotection by PlGF gene-modified human mesenchymal stem cells after cerebral ischaemia

H. Liu,[1] O. Honmou,[1,3,4] K. Harada,[1] K. Nakamura,[2] K. Houkin,[1] H. Hamada[2] and J. D. Kocsis[3,4]

Departments of [1]Neurosurgery and [2]Molecular Medicine, Sapporo Medical University School of Medicine, Sapporo, Japan, [3]Department of Neurology, Yale University School of Medicine, New Haven and [4]Neuroscience Research Center, VA Medical Center, West Haven, CT, USA

Correspondence to: Osamu Honmou, MD, Department of Neurosurgery, Sapporo Medical University School of Medicine, South-1st, West-16th, Chuo-ku, Sapporo, Hokkaido 060-8543, Japan
E-mail: honmou@sapmed.ac.jp

Intravenous delivery of mesenchymal stem cells (MSCs) prepared from adult bone marrow reduces infarction size and ameliorates functional deficits in rat cerebral ischaemia models. Placental growth factor (PlGF) is angiogenic to impaired non-neural tissue. To test the hypothesis that PlGF contributes to the therapeutic benefits of MSC delivery in cerebral ischaemia, we compared the efficacy of systemic delivery of human MSCs (hMSCs) and hMSCs transfected with a fibre-mutant F/RGD adenovirus vector with a PlGF gene (PlGF-hMSCs). A permanent middle cerebral artery occlusion (MCAO) was induced by intraluminal vascular occlusion with a microfilament. hMSCs and PlGF-hMSCs were intravenously injected into the rats 3 h after MCAO. Lesion size was assessed at 3 and 6 h, and 1, 3, 4 and 7 days using MR imaging and histology. Functional outcome was assessed using the limb placement test and the treadmill stress test. Both hMSCs and PlGF-hMSCs reduced lesion volume, induced angiogenesis and elicited functional improvement compared with the control sham group, but the effect was greater in the PlGF-hMSC group. Enzyme-linked immunosorbent assay of the infarcted hemisphere revealed an increase in PlGF in both hMSC groups, but a greater increase in the PlGF-hMSC group. These data support the hypothesis that PlGF contributes to neuroprotection and angiogenesis in cerebral ischaemia, and cellular delivery of PlGF to the brain can be achieved by intravenous delivery of hMSCs.

Keywords: angiogenesis; bone marrow transplantation; neural transplantation; regeneration; stroke

Abbreviations: BDNF = brain-derived neurotrophic factor; DWIs = diffusion-weighted images; ELISA = enzyme-linked immunosorbent assay; hMSCs = human MSCs; MCAO = middle cerebral artery occlusion; MOI = multiplicity of infection; MSCs = mesenchymal stem cells; PBS = phosphate-buffered saline; PlGF = placental growth factor; TTC = 2,3,5-triphenyltetrazolium chloride; TUNEL = terminal deoxynucleotidyltransferase dUTP nick-end labelling; VEGF = vascular endothelial growth factor

Received January 24, 2006. Revised and accepted June 1, 2006. Advance Access publication August 10, 2006.

Introduction

Transplantation of human mesenchymal stem cells (hMSCs) several hours after ischaemia onset can reduce infarction size and improve functional outcome in rodent cerebral ischaemia models (Chen *et al.*, 2001*a*; Li *et al.*, 2002; Iihoshi *et al.*, 2004, 2005; Nomura *et al.*, 2005; Honma *et al.*, 2006). Under appropriate conditions, mesenchymal stem cells (MSCs) can differentiate into cells of neuronal and glial lineage (Prockop *et al.*, 1997; Woodbury *et al.*, 2000; Kobune *et al.*, 2003, 2005; Nomura *et al.*, 2005; Honma *et al.*, 2006), but the beneficial effects of MSCs are not thought to result from neurogenesis. Rather, neuroprotective and angiogenic effects may be primarily responsible (Chen *et al.*, 2001*a*).

There is low-level basal secretion from hMSCs of several neurotrophic factors in culture, but ischaemic rat brain extracts induce production of neurotrophins and angiogenic growth factors (Chen *et al.*, 2002). One of these, brain-derived neurotrophic factor (BDNF), constitutively expressed at low level in primary hMSC cultures (Kurozumi *et al.*, 2004; Nomura *et al.*, 2005), increased in the ischaemic lesion following hMSC treatment in the rat middle cerebral artery occlusion (MCAO) model (Kurozumi *et al.*, 2004; Nomura *et al.*, 2005). Transplantation of BDNF gene-modified hMSCs resulted in stronger therapeutic effects with increased BDNF levels in the ischaemic lesion (Kurozumi *et al.*, 2004;

Nomura *et al.*, 2005). Thus, BDNF may play an important role in the therapeutic benefits on cerebral ischaemia following hMSC transplantation. The capacity of MSCs to release growth and trophic factors has been suggested to be the key to the beneficial effect in cerebral ischaemia (Chen *et al.*, 2002).

In addition to neurotrophic factors that may confer neuroprotective effects, isolated cultured bone marrow-derived stromal cells secrete angiogenetic cytokines, vascular endothelial growth factor (VEGF) and placental growth factor (PlGF) (Kinnaird *et al.*, 2004). These factors promoted the growth of new and stable vessels in cardiac and limb ischaemia (Luttun *et al.*, 2002*b*; Autiero *et al.*, 2003). While the administration of VEGF is reported to consist of both neuroprotective and angiogenic effects in the ischaemic brain (Sun *et al.*, 2003; Manoonkitiwongsa *et al.*, 2004), the role of the VEGF family member, PlGF (Malione *et al.*, 1991), on stroke therapy remains unclear. In this study, hMSCs and PlGF hypersecreting hMSCs (PlGF-hMSCs) were intravenously delivered at 3 h after induction of unilateral permanent cerebral ischaemia to investigate if cellular delivery of PlGF by hMSCs could influence structural integrity and functional outcome. We demonstrate that both cell types induce elevated PlGF levels in ischaemic brain and a concomitant reduction in lesion volume, increased angiogenesis and functional improvement. However, greater effects were observed with the PlGF-hMSC infusions. These results suggest that PlGF may be an important molecule in the therapeutic effects of hMSC treatment in cerebral ischaemia.

Material and methods

Preparation of human mesenchymal stem cells

hMSCs were processed for cell culture as described previously (Nomura *et al.*, 2005; Honma *et al.*, 2006). Briefly, human bone marrow from healthy adult volunteers was obtained by aspiration from the posterior iliac crest after informed consent was obtained; the subject's consent was obtained according to the Declaration of Helsinki, and this study was approved by the Institutional Review Board at our university. Bone marrow mononuclear cells were isolated and were plated in 150 cm^2 plastic tissue culture flasks and incubated overnight. After washing away the free cells, the adherent cells were cultured in Mesenchymal Stem Cell Basal Medium (MSCBM, Cambrex, Walkersville, Maryland, USA) containing Mesenchymal Cell Growth Supplement (MCGS, Cambrex), 4 mM L-glutamine, in a humidified atmosphere of 5% CO_2 at 37°C. After reaching confluency, they were harvested and cryo-preserved as primary MSCs or used for gene transduction.

Adenoviral vectors

Adenoviral vectors carrying a human PlGF cDNA were constructed on the basis of the method of Kurozumi *et al.* (2004) with minor modifications. Briefly, human PlGF cDNA was cloned using the reverse-transcription polymerase chain reaction (RT–PCR) method using the total RNA extracted from primary MSC as the template. The identity of PlGF cDNA obtained in this manner was confirmed by sequencing and comparing it with the GeneBank sequence NM_002632. The human PlGF primer sequence was forward, 5′-CGGAATTCCACCATGCCGGTCATGAGGCTGTTCCCT-3′, and reverse, 5′-CCAGATCTTACCTCCGGGGAACAGCATCGCC-3′.

The PlGF cDNA was inserted between the *Eco*RI site and the *Bgl* II site in the pCAcc vector and the resulting plasmid was designated pCAhPlGF. The plasmid pCAhPlGF was digested with *Cla* I, and the fragment containing the PlGF cDNA expression unit was isolated by agarose gel electrophoresis. The adenoviral PlGF expression vector, pWEAxCAhPlGF-F/RGD, was prepared using LipofectAMINE 2000 (Invitrogen, Tokyo, Japan).

Before being used, the above viral vectors were evaluated for their viral concentration and titre, and viral stocks were examined for potential contamination with replication-competent viruses. To determine viral concentration [particle unit (pu)/ml], the viral solution was incubated in 0.1% sodium dodecyl sulphate and A_{260} was measured. The viral titres of AxCAhPlGF-F/RGD were 1.0×10^{12} pu/ml.

Adenovirus infection

Adenovirus-mediated gene transfection was performed as described previously (Kurozumi *et al.*, 2004, 2005). Briefly, the cells were seeded at a density of 2×10^6 cells per 15 cm plate. hMSCs were exposed to the infectious viral particles in 7.5 ml DMEM at 37°C medium for 60 min; cells were infected with AxCAhPlGF-F/RGD or AxCALacZF/RGD at a multiplicity of infection (MOI) of 3.0×10^3 pu/cell. The medium was then removed, and the cells washed once with DMEM and then re-cultured with normal medium for 24 h, after which transplantation was performed.

Phenotypic characterization of the hMSC and hMSC-PlGF cells

Flow cytometric analysis of primary hMSCs and PlGF-hMSCs was performed as described previously (Honma *et al.*, 2006). Briefly, cell suspensions were washed twice with phosphate-buffered saline (PBS) containing 0.1% bovine serum albumin (BSA). For direct assays, aliquots of cells at a concentration of 1×10^6 cells per millilitre were immunolabelled at 4°C for 30 min with the following antihuman antibodies: fluorescein isothiocyanate (FITC) conjugated CD45, CD34 (Immunotech, Marseilles, France), and CD105 (SH-2) (Ancell, Bayport, MN, USA). As an isotype-matched control, mouse immunoglobulin G1-FITC (IgG1-FITC) (Immunotech, Marseille, France) was used. For indirect assays, cells were immunolabelled with antihuman CD73 (SH-3) (Alexis Biochemicals, San Diego, CA, USA). As the secondary antibody, goat anti-mouse IgG [heavy plus light (H plus L)]–FITC (Immunotech) was used. Labelled cells were analysed by a FACSCalibur flow cytometer (Becton Dickinson, San Jose, CA, USA) with the use of CellQuest software. Dead cells were gated out with forward- versus side-scatter window and propidium iodide staining.

Cerebral ischaemic model

The rat MCAO model was used as a stroke model. We induced permanent MCAO by using a previously described method of intraluminal vascular occlusion (Longa *et al.*, 1989). Adult male Sprague–Dawley rats (n = 151) weighing 230–250 g were initially anaesthetized with 5% isoflurane and maintained under anaesthesia with 1.5% isoflurane in a mixture of 70% N_2O and 30% O_2 with mechanical ventilation. Rectal temperature was maintained at 37°C with an infrared heat lamp. The left femoral artery was cannulated for measuring blood pH, pO_2, pCO_2 and blood pressure throughout the surgery. A length of 20.0–22.0 mm 4–0 surgical

dermalon suture with the tip rounded by heating near a flame was advanced from the external carotid artery into the lumen of the internal carotid artery until it blocked the origin of the MCA.

Transplantation procedures

Experiments consisted of three groups: Group 1, medium (MSCBM) alone (without donor cell administration) ($n = 51$), Group 2, hMSCs (1.0×10^7) ($n = 46$), and Group 3, PlGF-hMSCs (1.0×10^7) ($n = 45$). All injections were done 3 h after MCAO and cells were suspended in 1 ml of medium.

In some experiments, AxCALacZ-F/RGD adenovirus was used to transduce the LacZ gene into the hMSC ($n = 8$) and PlGF-hMSC ($n = 16$). Details of the construction procedures are described elsewhere (Niwa *et al.*, 1991; Nakamura *et al.*, 1994; Nakagawa *et al.*, 1998; Takiguchi *et al.*, 2000). For *in vitro* adenoviral infection, 1.0×10^7 MSCs were placed with AxCALacZ-F/RGD at an MOI of 3.0×10^3 pu/cell for 1 h and incubated at 37°C in a medium containing 10% foetal calf serum.

MRI studies and measurement of infarct volume

Rats were anaesthetized with ketamine (50 mg/kg) and xylazine (6 mg/kg) intraperitoneally. Each rat was placed in an animal holder/MRI probe apparatus and positioned inside the magnet. The animal's head was held in place inside the imaging coil. All MRI measurements were performed using a 7-T, 18-cm-bore superconducting magnet (Oxford Magnet Technologies, Witney, Oxfordshire, UK) interfaced to a UNITYINOVA console (Oxford Instruments, Witney, Oxfordshire, UK and Varian, Inc., Palo Alto, CA, USA). T_2-weighted images (T_2-WI) were obtained from a 1.0-mm-thick coronal section with a 0.5 mm gap using a 30 mm × 30 mm field of view, repetition time (TR) = 3000 ms, echo time (TE) = 37 ms, *b*-value = 0, and reconstructed using a 256 × 256 image matrix. Diffusion-weighted images (DWIs) were obtained at the same condition as T_2-WI except *b*-value (*b*-value = 1000). Accurate positioning of the brain was performed to centre the image slice 5 mm posterior to the rhinal fissure with the head of the rat held in a flat skull position. MRI measurements were obtained 3, 6, 24 h and 3, 4 and 7 days after MCAO.

The ischaemic lesion area was calculated from both T_2-WI and DWI using imaging software (Scion Image, Version Beta 4.0.2, Scion Corporation, Frederick, Maryland, USA), based on the previously described method (Neumann-Haefelin *et al.*, 2000). For each slice, the higher intensity lesions in both T_2-WI and DWI where the signal intensity was 1.25 times higher than the counterpart in the contra-lateral brain lesion were marked as the ischaemic lesion area, and infarct volume was calculated taking slice thickness (1 mm/slice) into account.

Detection of PlGF *in vitro* and *in vivo*

Forty-eight hours after hMSCs were transfected *in vitro* at various MOI (pu/cell), culture supernatants were collected for analysis. Furthermore, three and seven days after MCAO, rats were anaesthetized with ketamine and xylazine intraperitoneally, their brains were removed and coronal sections (30 mg) from −0.3 to 1.3 mm to bregma in the ischaemic hemisphere were dissected on ice and were stored at −80°C until use. Subsequently, each tissue sample was suspended in an equal weight of homogenate buffer (1 ml; 137 mM NaCl, 20 mM Tris, 1% NP-40, 1 mM PMSF, 10 μg/ml aprotinin, 1 μg/ml leupeptin, 0.5 mM sodium vanadate) and homogenized with a Dounce homogenizer. The homogenate was centrifuged (10 000 *g*) for 10 min at 4°C, and the supernatant (1 μg/μl) was collected for analysis. Commercial PlGF ELISA (enzyme-linked immunosorbent assay) kits (R&D Systems Inc., Minneapolis, USA) were used to quantify the concentration of PlGF in each of the samples.

TTC staining and quantitative analysis of infarct volume

One week after transplantation, the rats were deeply anaesthetized with sodium pentobarbital (50 mg/kg, i.p.). The brains were removed carefully and dissected into coronal 1 mm sections using a vibratome. The fresh brain slices were immersed in a 2% solution of 2,3,5-triphenyltetrazolium chloride (TTC) in normal saline at 37°C for 30 min.

The cross-sectional area of infarction in each brain slice was examined with a dissection microscope and was measured using an image analysis software, NIH image. The total infarct volume for each brain was calculated by summation of the infarcted area of all brain slices.

Detection of donor PlGF-hMSCs *in vivo*

Two weeks after transplantation, the LacZ-transfected PlGF-hMSCs *in vivo* were detected using laser scanning confocal microscopy. Brains of the deeply anaesthetized rats were removed, fixed in 4% paraformaldehyde in phosphate buffer, dehydrated with 30% sucrose in 0.1 M PBS for overnight and frozen in powdered dry ice. Coronal cryostat sections (10 μm) were processed for immunohistochemistry. To identify the transplanted cells, LacZ-labelled PlGF-hMSCs were visualized with the use of antibody to β-galactosidase (rhodamine-labelled polyclonal rabbit anti-β-galactosidase antibody, DAKO, Carpinteria, CA, USA). To identify the cell type derived from the donor PlGF-hMSCs, double-labelling studies were performed with the use of antibodies to neurons (FITC-labelled monoclonal mouse NeuN, DAKO), astrocytes [FITC-labelled monoclonal mouse anti-glial fibrillary acidic protein (GFAP), Sigma, St Louis, MO, USA], oligodendrocytes (FITC-labelled monoclonal mouse anti-O4, Boehringer–Mannheim, Manheim, Germany), and endothelial cells [FITC-labelled polyclonal rabbit anti-von Willbrand factor (vWF), DAKO]. To excite the FITC fluorochrome (green), a 488 nm laser line generated by an argon laser was used, and for the Rhodamine fluorochrome (red), a 543 nm laser line from a HeNe laser was used. Confocal images were obtained using a Zeiss laser scanning confocal microscope with the use of Zeiss software.

TUNEL staining

Seven days after MCAO, rats were anaesthetized and transcardially perfused with PBS followed by 4% paraformaldehyde in PBS. Their brains were harvested and immersed in 4% paraformaldehyde in PBS for 2 days, after which 12 μm frozen sections were cut with a cryostat at −20°C. Cellular DNA fragmentation in the ischaemic boundary zone was detected using the TUNEL (terminal deoxynucleotidyltransferase dUTP nick-end labelling) method by means of an *in situ* Apoptosis Detection Kit (TaKaRa Biomedicals, Shiga, Japan). Specifically, after proteinase digestion, the sections were incubated in a mixture containing terminal deoxynucleotidyltransferase and FITC-labelled dUTP. Sections were counterstained with propidium iodide. The number of TUNEL-positive cells was counted in three 651.5 μm × 651.5 μm regions of the boundary zone.

Three-dimensional image acquisition for angiogenesis

Seven days after MCAO, rats were anaesthetized and intravenously perfused with FITC dextran (1 ml, Sigma). The brains were immediately removed, and were fixed in 4% paraformaldehyde at 4°C for 48 h. Coronal vibratome sections (100 μm) were analysed with a laser scanning confocal imaging system (LSM Pascal; Carl Zeiss, Jend, Germany). The sections were scanned in 512 × 512 pixel (651.5 μm × 651.5 μm) format in the x–y direction using a 5× frame-scan average (2.18 μm interval and 2.4 μm thickness along the z-axis) under a 20× objective. Vessel volumes were measured in the three dimensions using the software of Zeiss LSM.

Treadmill stress test

Rats were trained 20 min per day for 2 days a week to run on a motor-driven treadmill at a speed of 20 m/min with a slope of 0°C. Rats were placed on a moving belt facing away from the electrified grid and induced to run in the direction opposite of the movement of the belt. Thus, to avoid foot-shocks (with intensity in 1.0 mA), the rats had to move forward. Only the rats that had learned to avoid the mild electrical shock were included in this study. The maximum speed at which the rats could run on a motor-driven treadmill was recorded.

Limb placement test (LPT)

The rats' four limbs were evaluated using the top and edges of a counter top (Ohlsson *et al.*, 1995). Each test was scored as follows: 0, no placing; 1, incomplete and/or delayed (>2 s) placing; and 2, immediate and correct placing. For each body side, the maximum score from the tests used was 16. The forepaws were graded in all six tests; in tests 4 and 6, the hind limbs were also tested. During tests 1 through 4, the rat was held in a soft grip by the examiner. In test 1, limb placing was tested by slowly lowering the rat toward a table. At ~10 cm above the table, normal rats stretch and place both forepaws on the table. For test 2, with the rat's fore limbs touching the table edge, the head of the rat was moved 45° upward while the chin was supported to prevent the nose and the vibrissae from touching the table. A rat with focal brain lesion may lose contact with the table with the paw contra-lateral to the injured hemisphere. In test 3, fore limb placement of the rat when facing a table edge was observed. A normal rat places both forepaws on the table top. Test 4 recorded fore limb and hind limb placement when the lateral side of the rat's body was moved toward the table edge. For test 5, the rat was placed on the table and gently pushed from behind toward the table edge. A normal rat will grip on the edge, but an injured rat may drop the fore limb contra-lateral to the injured hemisphere. Test 6 was the same as test 5, but the rat was pushed laterally toward the table edge.

Statistical analysis

Data are presented as mean values ± standard deviation, and were statistically analysed. Differences among groups were assessed by ANOVA (analysis of variance) with Scheffe's *post hoc* test to identify individual group differences. Differences were deemed statistically significant at $P < 0.05$.

Results

Characteristics of primary and PlGF gene-transduced hMSCs

Primary hMSCs were cultured as plastic adherent cells to subconfluency ~1 week (*see* Material and methods). A characteristic feature of hMSCs is a $CD34^-$, $CD45^-$, $SH2^+$(CD105), $SH3^+$(CD73) cell surface phenotype (Kobune *et al.*, 2003). Both flattened and spindle-shaped cells can be recognized in the culture. PlGF-hMSCs showed similar flattened and spindle-shaped morphology. Flow cytometric analysis of the PlGF-hMSCs (Fig. 1B) was essentially identical to primary hMSCs (Fig. 1A).

Detection of immunoreactive human PlGF and quantitative analysis *in vitro*

Levels of PlGF in the supernatant of cultured hMSCs and PlGF-hMSCs with different MOI levels were studied. hMSC transfected with AxCAhPlGF-F/RGD (PlGF-hMSC) at an MOI of 300, 1000 and 3000 pu/cell secreted PlGF at a rate of 0.72 ± 0.33, 2.19 ± 0.36 and 7.57 ± 1.14 ng/10^5 cells/48 h, respectively ($n = 6$). Non-transfected hMSC also produced PlGF protein (0.025 ± 0.002 ng/10^5 cells/48 h) ($n = 6$). AxCALacZ-F/RGD at an MOI of 3000 pu/cell secreted PlGF at a rate of 0.02 ± 0.004 ng/10^5 cells/48 h ($n = 6$). These data are summarized in Fig. 1C. The level of PlGF production from PlGF-hMSC transfected at an MOI of 3000 pu/cell was ~300-fold greater than that seen in non-infected or LacZ-infected hMSC.

Characterization of ischaemic lesion size by magnetic resonance image analysis

An estimate of lesion size was obtained using *in vivo* MRI (*see* Material and methods). The cells were intravenously delivered immediately after the 3 h MRI. DWI and T_2-WI are shown in Fig. 2A and B, respectively. These coronal forebrain sections were obtained at the level of caudato-putamen complex. Images obtained at 3 h (column 1), 3 days (column 2) and 7 days (column 3) are shown for control (medium) ($n = 10$), hMSC ($n = 9$) and PlGF-hMSC-injected groups ($n = 8$) (Fig. 2). The reduction in density in lesions on the right side of the brains that were subjected to ischaemic injury may be noted. Lesion volume (mm^3) was determined by analysis of high-intensity areas on serial images collected through the cerebrum (*see* Material and methods).

As calculated from the DWI the lesion volume at 3 h after MCAD was similar in the control, hMSC and the PlGF-hMSC groups (Fig. 3A). In order to determine the efficacy of hMSC or PlGF-hMSC transplantation in modulating the ischaemic lesion volume, 1×10^7 cells were delivered intravenously at 3 h after MCAO, and animals were re-imaged at 6 and 24 h, 3, 4 and 7 days later. In the sham control group, MRI-estimated lesion volume reached maximum at 3 days, and gradually decreased at Day 4, and at 7 days post-MCAO. Although lesion volumes estimated 3 h after MCAO were the same among the three groups, lesion volume was smaller 6 h after MCAO in the PlGF-hMSC-treated group (Fig. 3A). However, at 24 h, 3, 4 and 7 days, lesion volume was less in both hMSC and PlGF-hMSC groups as compared with control. The reduction in lesion volume was greater for the PlGF-hMSC group as compared with the hMSC group

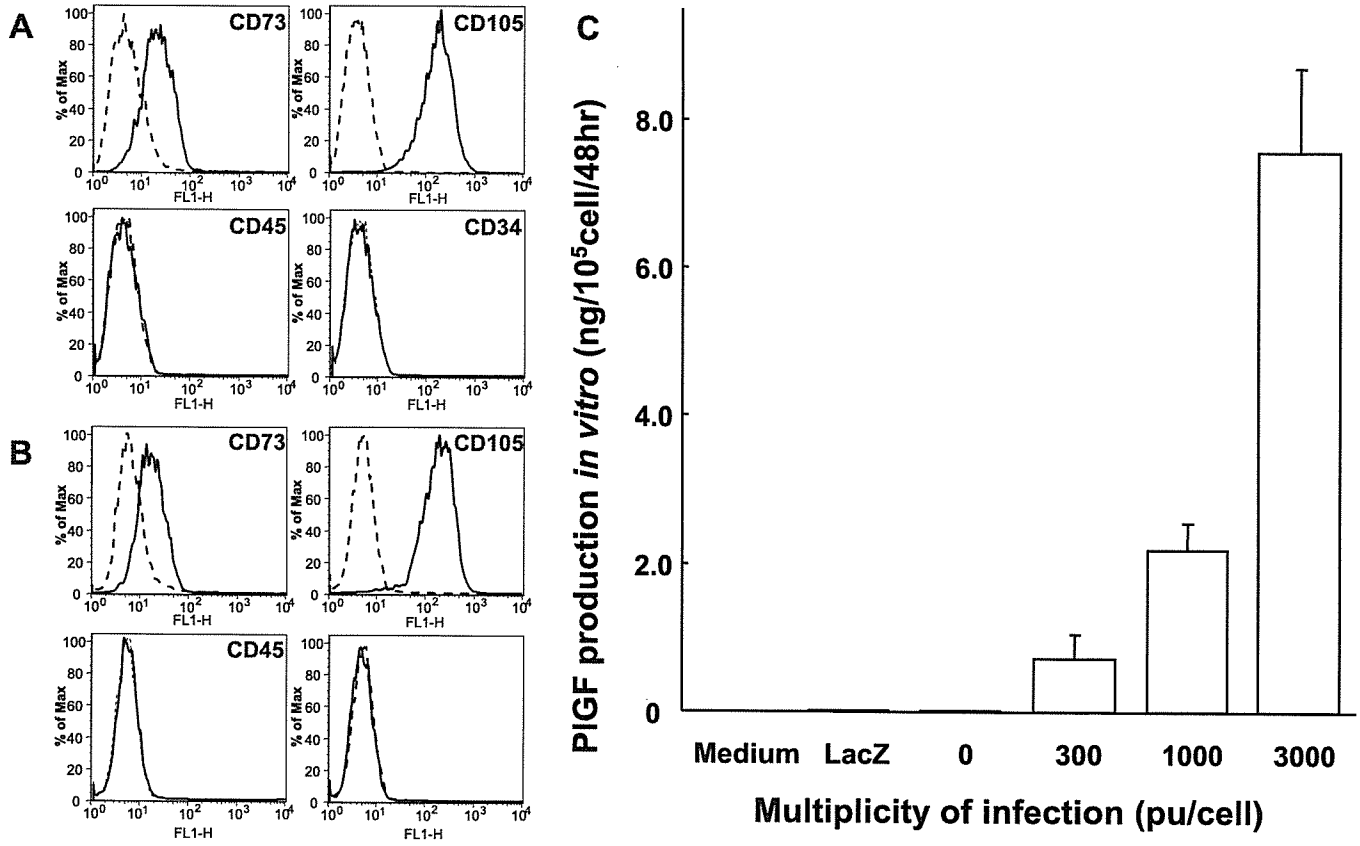

Fig. 1 Flow cytometric analysis of surface antigen expression on primary hMSC (**A**) and PlGF-hMSC (**B**). The cells were immunolabelled with FITC-conjugated monoclonal antibody specific for the indicated surface antigen. Dead cells were eliminated by forward and side scatter. PlGF production of hMSC, LacZ-transfected hMSC and PlGF-transfected hMSC were summarized (**C**). Levels of PlGF in the supernatant were shown.

at 3, 4 and 7 days post-MCAO. These results are summarized in Fig. 3A. Lesion volume estimated from T_2-WI showed similar results as with the DWI (Fig. 2B and 3B).

Histological determination of infarction volume

A second independent measure of infarction volume was performed. The brains were stained with TTC 7 days after MCAO (Fig. 4A). Normal brain (grey matter) tissue typically stains with TTC, but infarcted lesions show no or reduced staining (Bederson *et al.*, 1986). TTC staining obtained 7 days after MCAO without cell transplantation is shown in Fig. 4A-1. The reduced staining on the lesion side may be noted. Lesion volume was calculated by measuring the area of reduced TTC staining in the forebrain ($n = 5$) (*see* Material and methods). As with MRI analysis there was a reduction in infarction volume with both hMSC ($n = 5$) (Fig. 4A-2) and PlGF-hMSC ($n = 5$) (Fig. 4A-3) treatment, but the effect of PlGF-hMSC was larger. Intravenous delivery of 1×10^7 PlGF-hMSCs resulted in very substantial reduction in lesion volume as estimated from TTC staining (Fig. 3C). We have shown in a previous paper (Kurozumi *et al.*, 2005) that hMSCs transfected with AxCAhEGFP-F/RGD directly injected into the brain of MCAO rats did not show increased neuroprotection as compared with cells transfected to express various cytokines.

Identification and characterization of donor cells *in vivo*

LacZ-transfected PlGF-hMSCs that had been intravenously administered (10^7 cells) 3 h after MCAO were identified *in vivo* ($n = 16$). The LacZ-expressing PlGF-hMSCs were found primarily in the lesion penumbra. Immunohistochemical studies were carried out to identify LacZ-positive cells in and around the lesion zone in animals transplanted with LacZ-transfected PlGF-hMSCs (Fig. 4B and C). The numbers of LacZ-positive cells were obtained from one section per rat, and four separate rats ($n = 4$) were analysed, demonstrating a large number of LacZ-positive cells in and around the lesion (74.00 ± 23.10 cells/mm^2, $n = 4$), although virtually no LacZ-positive cells were observed in the non-damaged hemisphere and non-infected group. A small number of the LacZ-positive donor cells expressed the NeuN (10.53 ± 3.43%, $n = 4$) (Fig. 4B), or GFAP (17.23 ± 4.00%, $n = 4$) (Fig. 4C), and very few of LacZ-positive cell population were O4-positive ($n = 4$). Moreover, only a small fraction of cells estimated from LacZ cell counts can reach the lesion in the brain, which is similar to previous studies (Chen *et al.*,

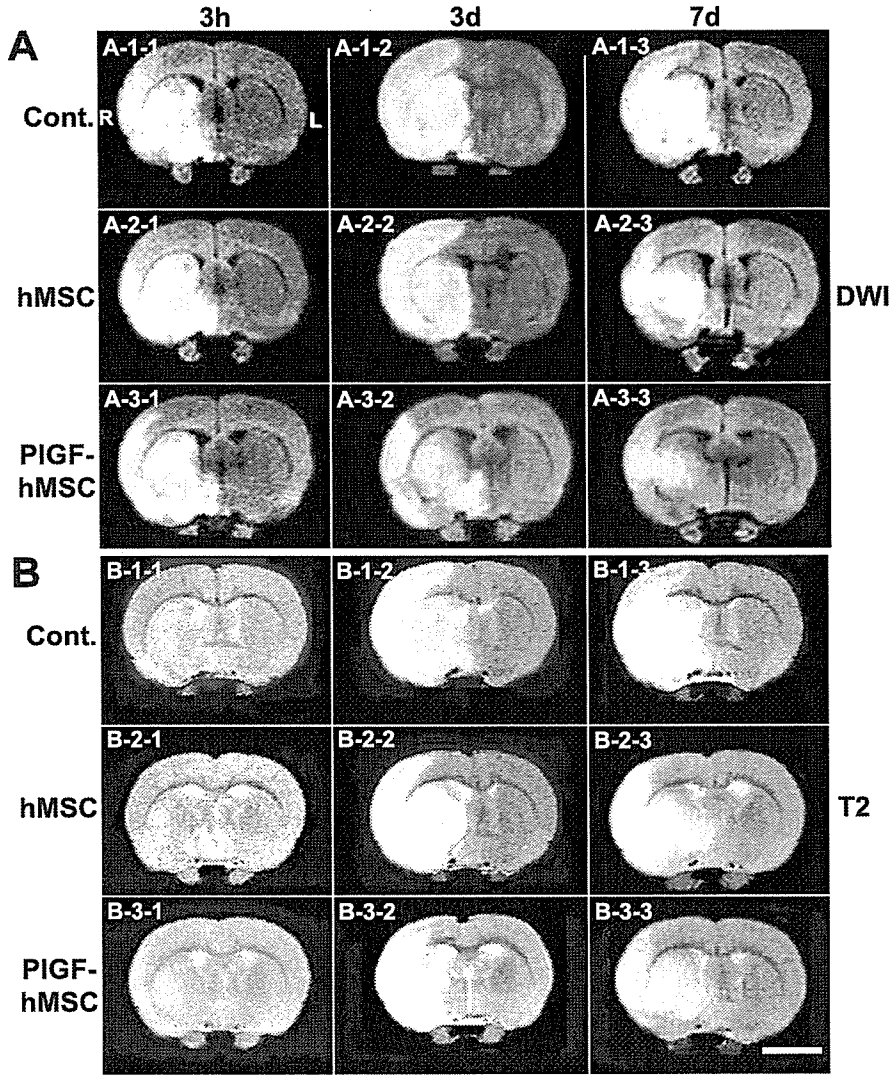

Fig. 2 DWI- and T_2-weighted images (T_2), collected at 3 h (column 1), 3 days (column 2) and 7 days (column 3) post-lesion induction. The 3 h images were obtained just before intravenous cell or vehicle injection. Images from sham control, hMSC and PlGF-hMSC injections are shown in rows 1, 2 and 3, respectively, for data sets of (**A**) DWI and (**B**) T_2. The infarction is observed as a high-intensity area of the ischaemic (right) side of the brain. Scale bar = 5 mm.

2001*b*; Li *et al.*, 2001; Inoue *et al.*, 2003). The density of LacZ-positive cells estimated from the immunohistochemical analysis was ~500 cells/mm^3 in the ischaemic core and ~7400 cells/mm^3 in the boundary zone. Infarcted volume ranged from 150 to 250 mm^3. The number of intravenously injected cells was 10^7 cells. Thus, the minimum percentage of intravenously injected cells accumulating in the ischaemic core was ~0.75%, and the maximum number in the boundary zone was ~18.5%.

PlGF levels *in vivo*

PlGF levels in focal brain tissue were measured by a sandwich ELISA 3 and 7 days after MCAO (*see* Material and methods). PlGF levels significantly increased in the ischaemic hemisphere of the hMSC-treated group (n = 10) compared with control group (n = 10) at 3 and 7 days after MCAO (Fig. 3D). In the PlGF-hMSC-treated rats (n = 10), PlGF increased in the ischaemic hemisphere to a greater extent than the hMSC-treated rats. It may be noted that the PlGF levels also significantly increased in the medium-treated group compared with the normal brain (n = 10). In the PlGF-hMSC groups, PlGF levels were similar at 47.7 ± 10.4 pg/mg on Day 3 versus 40.8 ± 3.5 pg/mg (n = 5, P = 0.22). Thus, PlGF secretion in the PlGF-hMSC group was above control and the hMSC group for at least a week after cell infusion. These results are summarized in Fig. 3D.

Reduced nuclear DNA fragmentation in treated animals

Nuclear DNA fragmentation was studied in the ischaemic boundary zone. There were significantly fewer TUNEL positive cells in animals treated with hMSC in the ischaemic

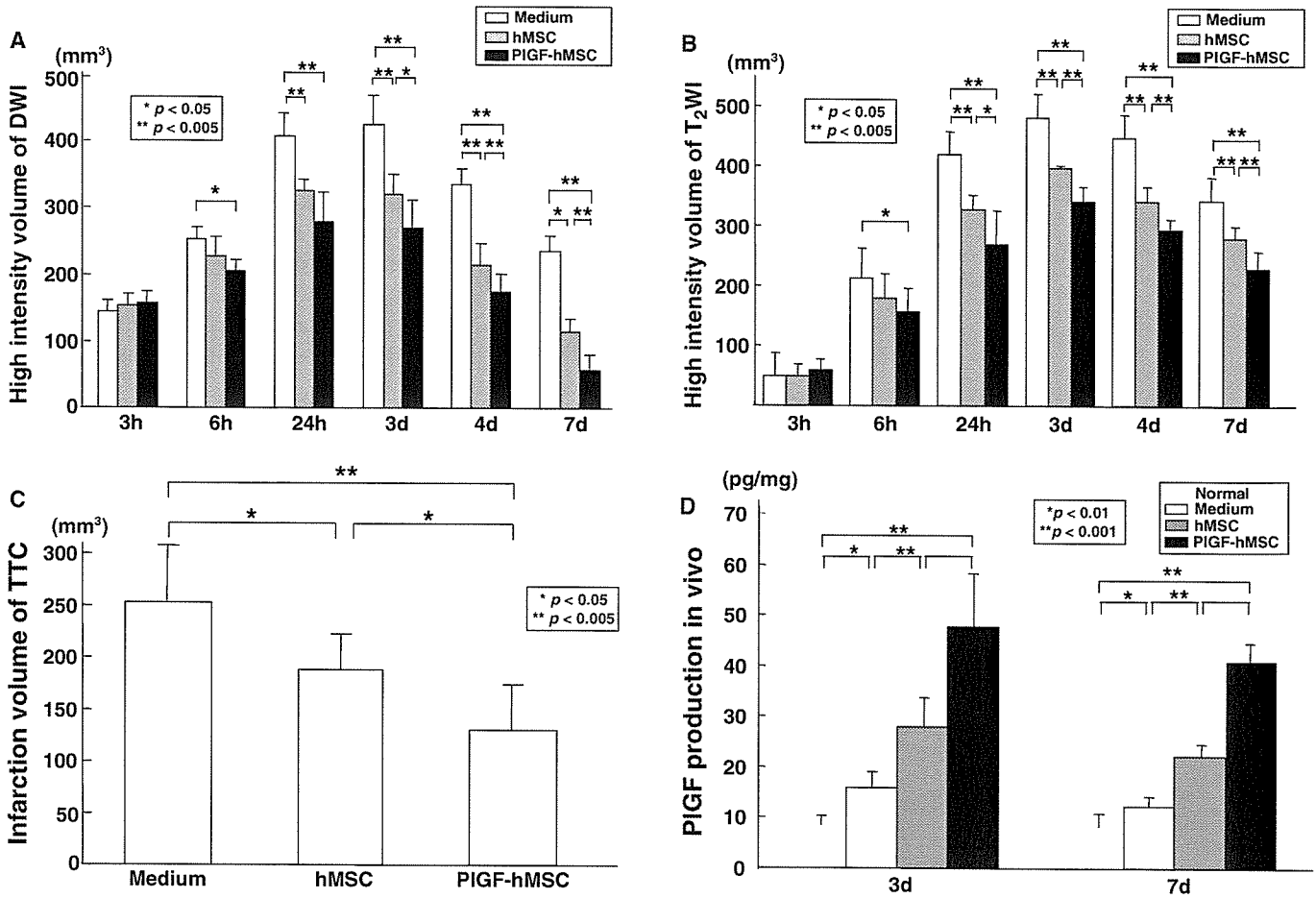

Fig. 3 A summary of lesion volumes evaluated with MRI (DWI) (**A**), T_2-WI (**B**) and TTC staining (**C**). Both DWIs (**A**) and T_2-WIs (**B**) were obtained 3, 6 and 24 h, 3, 4 and 7 days after MCAO in rats treated with medium (control), hMSC or PIGF-hMSC. Images at 3 h were obtained just before treatment. (**C**) Seven days after MCAO, there was a reduction in the lesion volume assayed using TTC staining for both hMSC and PIGF-hMSC groups, but the reduction was greater in the PIGF-hMSC group. (**D**) PIGF *in vivo* levels assayed with ELISA. Levels of PIGF were significantly increased in the ischaemic hemisphere of hMSC and PIGF-hMSC compared with medium-treated rats. In addition, PIGF levels were greater in the ischaemic hemisphere of PIGF-hMSC-transplanted as compared with rats that received hMSC. Assays were obtained 3 and 7 days after MCAO induction. Note that PIGF was increased in the lesion with medium injection alone.

boundary zone 7 days after MCAO (24.25 ± 5.78 cells/mm^2, $n = 4$; $P < 0.01$) (Fig. 5A-3) compared with those treated with medium (123.00 ± 33.25 cells/mm^2, $n = 4$) (Fig. 5A-2). The reduced apoptotic cell death is more obvious in the PlGF-hMSC-treated group (11.50 ± 4.44 cells/mm^2, $n = 4$; $P < 0.05$) compared with those in the hMSC-treated group (Fig. 5A-4). Figure 5A-1 indicated that there is no apoptotic cell in the normal rat brain ($n = 4$). These results were summarized in Fig. 5B.

Angiogenesis introduced by the transplantation

To examine whether the administration of hMSCs and PlGF-hMSCs induces angiogenesis, three-dimensional analysis of capillary vessels in the lesion was performed using Zeiss LSM5 PASCAL software. Figure 6A-1 shows the three-dimensional capillary image in the normal rat brain ($n = 4$). The capillary vascular volume in the boundary region 7 days after MCAO was increased in the hMSC-treated group ($n = 4$) (Fig. 6A-3) compared with the medium-treated group ($n = 4$) (Fig. 6A-2), and the angiogenesis was greater in the PlGF-hMSC-treated group ($n = 4$) (Fig. 6A-4). The capillary vascular volume was expressed as a ratio by dividing that obtained from the ischaemic hemisphere by that of the contra-lateral control hemisphere. The ratio was significantly higher in both the hMSC (0.48 ± 0.13; $P < 0.05$) and the PlGF-hMSC (1.37 ± 0.33; $P < 0.001$) treated groups as compared with the medium-treated group (0.25 ± 0.02). These results were summarized in Fig. 6B.

Immunohistochemical studies were carried out to show endothelial cell differentiation of LacZ-positive cells in the lesion zone in animals transplanted with LacZ-transfected PlGF-hMSCs (Fig. 7). The vWF-positive cells in the boundary region 7 days after MCAO were increased in the hMSC-treated group ($n = 4$) compared with the medium-treated

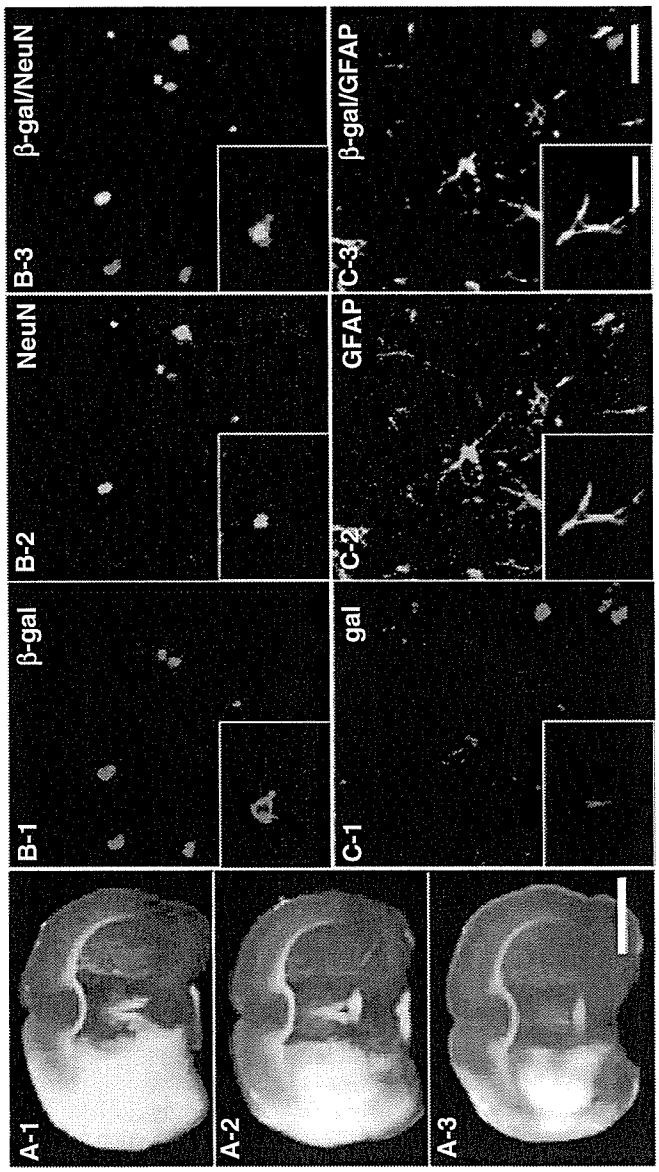

Fig. 4 Brain sections stained with TTC to visualize the ischaemic lesions 7 days after MCAO. Sections from non-treated MCAO (**A-1**), hMSC- (**A-2**) and PlGF-hMSC-treated (**A-3**) groups. Intravenously administrated PlGF-hMSCs accumulated in the ischaemic lesions (**B-1**, **C-1**). Confocal images show the differentiation of the transplanted cells (LacZ in red; **B-1** and **C-1**) into neurons (NeuN in green; **B-2**) or astrocytes (GFAP in green; **C-2**). NeuN localizes primarily in the nucleus. Panels **B-3** and **C-3** confirm the co-labelling of LacZ/NeuN or LacZ/GFAP in the cells, respectively. Higher power confocal images are shown in insets. Scale bar = 5 mm (**A**), 50 μm (**B** and **C**) and 30 μm (inserts).

group (n = 4), which was the greatest in the PlGF-hMSC-treated group (n = 4) (Fig. 7C). Double-positive cells of vWF and LacZ were also increased in the PlGF-hMSC-treated group compared with the hMSC-treated group (Fig. 7D).

Functional analysis

To assess behavioural performance in the lesioned and transplanted animals, the LPT and the treadmill stress test were performed before ischaemia onset, 3 and 24 h, 3, 4 and 7 days after MCAO. Before MCAO, LPT neurological scores were similar among all animals. Three hours after MCAO, but before transplantation, there was equal deficit in limb placement score among control ($n = 7$), hMSC-treated ($n = 7$) and PlGF-hMSC-treated group ($n = 7$) (Fig. 8A). LPT showed the lowest score in the sham-injected animals 24 h after MCAO with gradual improvement up to 7 days. In the hMSC transplantation group, the improvement in score was greater over the time course up to 7 days. PlGF-hMSC-treated group achieved a higher score at 3, 4 and 7 days as compared with hMSC-treated group. These results are summarized in Fig. 6A.

An independent behaviour study (treadmill stress test) was carried out. Before MCAO, there was no significant difference among control (n = 7), hMSC-treated (n = 7) and PlGF-hMSC-treated groups (n = 7) (Fig. 8B), and at 3 h post-MCAO there was comparable impairment among three groups. Twenty-four hours after MCAO maximum velocity on the treadmill test was at its maximum deficit. An increase in maximum velocity was observed for the PlGF-hMSC group at 24 h. Both hMSC and PlGF-hMSC groups had greater maximum velocity from 3 to 7 days than sham control, but the PlGF-hMSC group attained a higher velocity than the hMSC group. These results are summarized in Fig. 8B.

Discussion

The present study demonstrates that intravenous infusion of either hMSCs or PlGF-hMSCs 3 h after permanent MCAO in the rat results in an increase in PlGF levels in the infarcted cerebral hemisphere, reduction in infarction volume and apoptosis, induced angiogenesis and improvement in behavioural performance. These results are consistent with previous studies showing beneficial effects of bone marrow cell transplantation in experimental cerebral ischaemic models (Chen *et al*, 2001*b*; Iihoshi *et al.*, 2004; Nomura *et al.*, 2005; Honma *et al.*, 2006). While both hMSCs and PlGF-hMSCs showed efficacy, the effects, including brain PlGF levels, were greater in the PlGF-hMSC group.

The PlGF gene was introduced into hMSC, and an elevated secretion of PlGF protein as compared with non-transgenic hMSC was confirmed *in vitro* using ELISA. This relatively high secretory rate was achieved by using Ad-F/RGD, which has a higher transfection rate (Nakamura *et al.*, 2002; Tsuda *et al.*, 2003). PlGF levels in the ischaemic brain lesion assayed by ELISA increased after either hMSC or PlGF-hMSC delivery, but levels were significantly higher in the PlGF-hMSC group. This suggests that the PlGF-hMSC could maintain high levels of PlGF *in vivo* during the critical post-ischaemic period and that this elevated PlGF secretion contributes to the enhanced neuroprotection.

Attenuation of PlGF production by viral dilution could occur through cell division *in vivo*. We estimate that several copies of adenovirus were transfected into a single hMSC. Doubling time of hMSC is ~5 days. Therefore, in the present

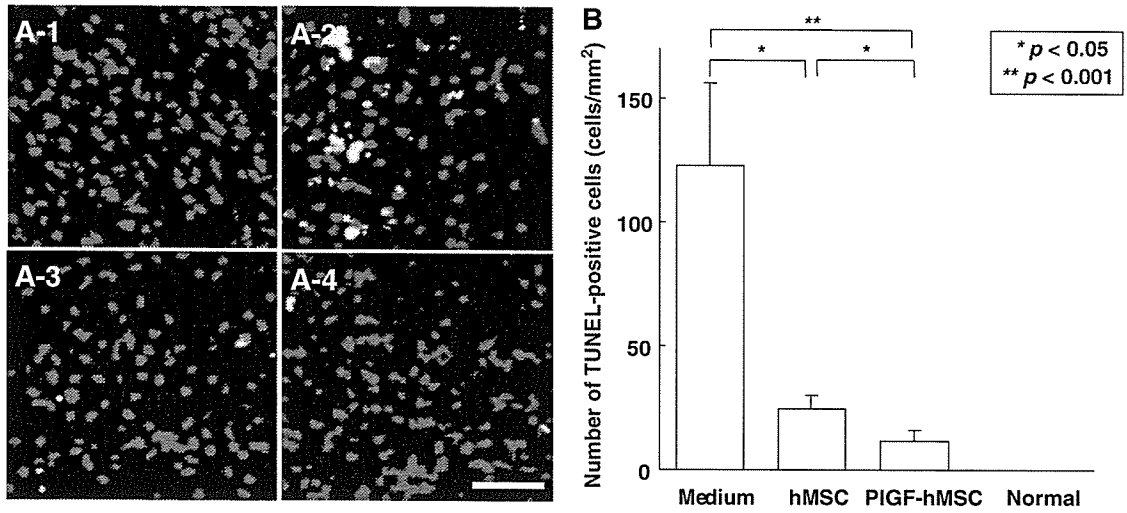

Fig. 5 Cells with DNA fragmentation were present in the ischaemic penumbra 7 days after MCAO. Fewer TUNEL-positive cells were detected in rats treated with PlGF-hMSCs (**A-4**) than those in hMSC-treated animals (**A-3**) and medium-treated animals (**A-2**) in the ischaemic boundary zone (yellow, TUNEL-positive: red, nuclear stain). Normal brain showed no TUNEL-positive cell (**A-1**). These results are summarized in **B**. Scale bar = 100 μm (**A**).

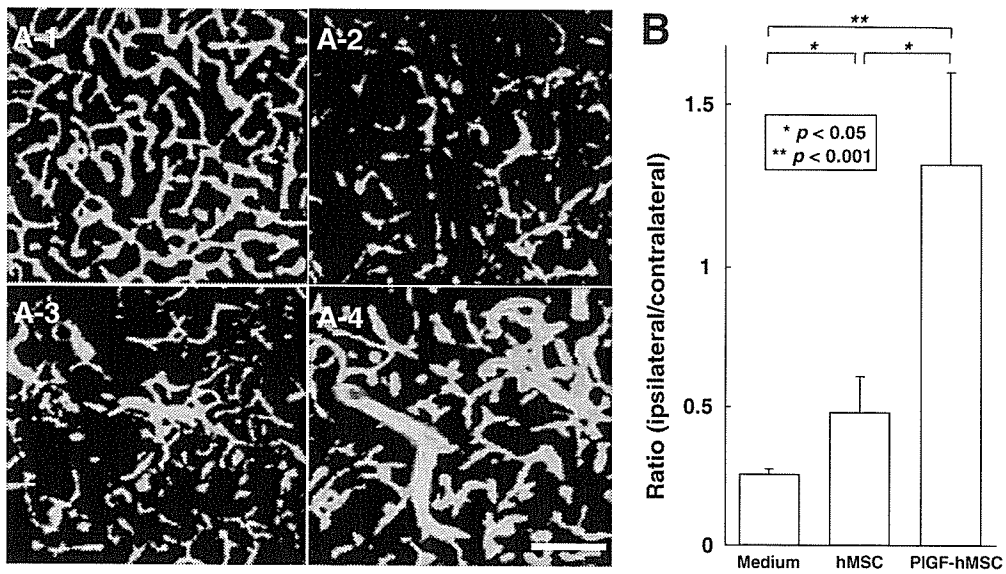

Fig. 6 Seven days after MCAO, the angiogenesis in boundary zone was analysed using a three-dimensional analysis system. **A-1** shows the three-dimensional capillary image with systemically perfused FITC-dextran in the normal rat brain. The total volume of the microvessels in the sampled lesion site decreased 7 days after MCAO (**A-2**), but was greater in the hMSC-treated group (**A-3**), and greater still in the PlGF-hMSC-treated group (**A-4**). These results are summarized in **B**. Scale bar = 150 μm (**A**).

study, hMSC may have divided one or two times *in vivo* after transplantation. Only one copy of virus in an hMSC can produce significant levels of PlGF. Therefore, PlGF production is not severely weakened for a week in our experimental paradigm, which is supported by the *in vivo* data in Fig. 3D. Also, the adenovirus vector used in the present study is composed of a ubiquitously strong promoter based on the β-actin promoter (Niwa *et al.*, 1991), which allowed strong expression in a variety of cell types. Neuroprotective and angiogenic effects that we expect from insertion of the PlGF gene require expression for perhaps several days. Prolonged expression of PlGF may cause unexpected side-effects. Therefore, transient expression may be sufficient and appropriate. Thus, even if some cell division occurs *in vivo*, it should not impede PlGF expression in the early critical period.

VEGF is an angiogenic and vascular permeability factor that exerts an acute neuroprotective effect in the ischaemic brain, and these effects operate independently (Sun *et al.*, 2003; Manoonkitiwongsa *et al.*, 2004). Although PlGF is a member of the VEGF family of growth factors (Maglione

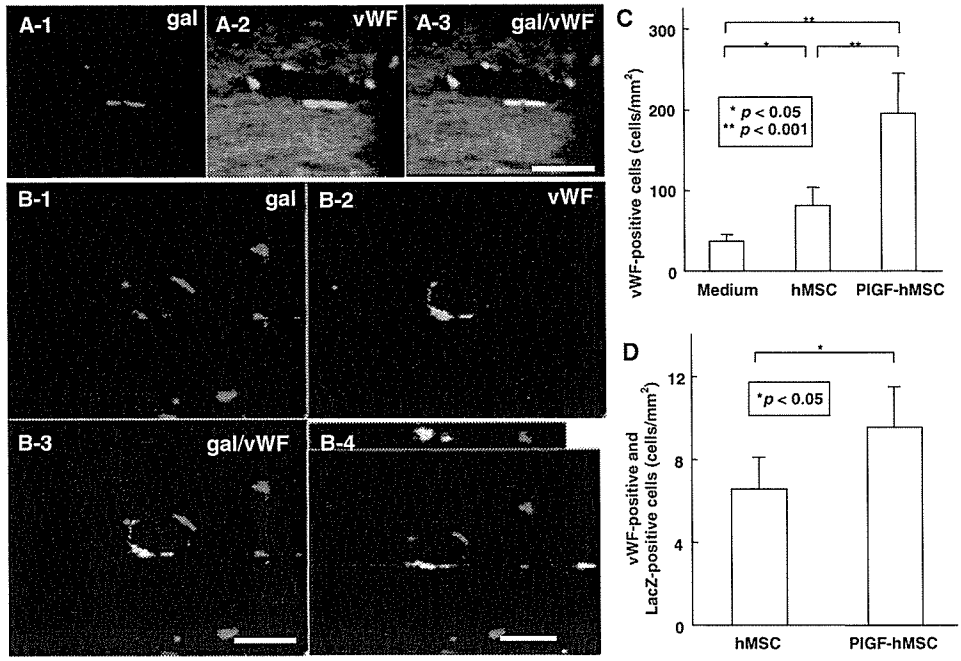

Fig. 7 Intravenously administrated PlGF-hMSCs differentiated into the endothelial lineage. Confocal images show the transplanted cells (LacZ in red; **A-1**, **B-1**) and endothelial cells (vWF in green; **A-2**, **B-2**). **A-3** and **B-3** confirm the co-labelling of LacZ/vWF in the cells. **B-4** also demonstrates z-axis projections of the image. The cell density of vWF-positive cells is shown in **C**. **D** demonstrates the cell density of vWF-positive cells co-localized with LacZ. Scale bar = 50 μm (**A** and **B**).

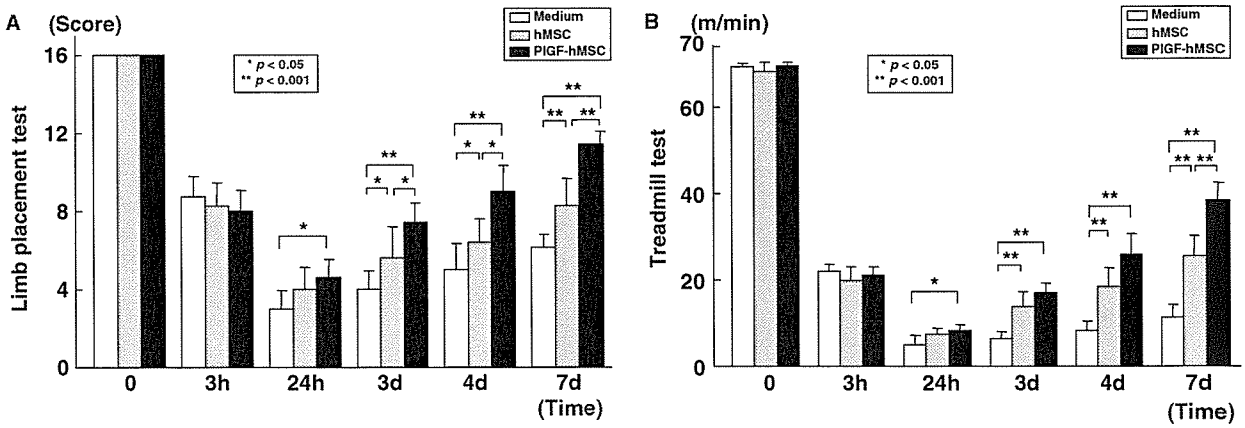

Fig. 8 Assessment of brain ischaemia-induced functional deficits using an LPT (**A**) and the treadmill stress test (**B**). Three hours after MCAO, but before intravenous cell delivery, there was no statistical difference in limb placement score among three groups. Twenty-four hours after MCAO, rats that received PlGF-hMSC achieved significantly higher limb placement scores compared with control rats. From 3 days on both hMSCs and PlGF-hMSCs showed greater functional improvement than medium alone, but the PlGF-hMSC group showed more improvement than the hMSC group. (**B**) The treadmill stress test demonstrates that the maximum speed at which the rats could run on a motor-driven treadmill was faster in the hMSC and the PlGF-hMSC-treated rats than control. Twenty-four hours after MCAO, rats that received hMSC-PlGF showed higher running speed compared with the medium alone, and the hMSC group. From three days on after MCAO, the hMSC and PlGF-hMSC groups attained higher velocities but the PlGF-hMSC group was greater. The highest level of functional improvement was attained at 7 days for both functional tests.

et al., 1991), less attention has been devoted to the therapeutic potential of PlGF for angiogenic disorders (De Falco *et al.*, 2002). However, recent work is focusing attention on PlGF (Luttun *et al.*, 2002*a*). PlGF gene transfer into ischaemic myocardium and limb caused pre-existing vessels to enlarge, resulting in tortuous, thin-walled, pericyte-poor 'mother' vessels (Luttun *et al.*, 2002*a*). The latter vessels remained enlarged and subsequently stabilized into mature, durable vessels by acquisition of a pericyte coat and, occasionally, by deposition of a thin rim of perivascular collagen. These vessels remained functional and persisted for >1 year after PlGF gene transfer (Carmeliet *et al.*, 2001). PlGF avoided

the harmful complications of VEGF such as oedema, fibrin deposition and growth of unstable vascular tangles and glomeruloid bodies in the impaired myocardium (Dvorak *et al.*, 1979; Pettersson *et al.*, 2000; Luttun *et al.*, 2002a).

Although PlGF is reported to have angiogenic effects in the impaired myocardium, limb and skin (Dvorak *et al.*, 1979; Pettersson *et al.*, 2000; Carmeliet *et al.*, 2001; Luttun *et al.*, 2002*b*), its effects on ischaemic brain had not been studied. However, upregulation of endogenous PlGF in ischaemic brain tissue was reported on both the mRNA and protein level (Beck *et al.*, 2002; Hayashi *et al.*, 2003), suggesting that PlGF may play an important role in endogenous repair or neuroprotection in the ischaemic lesion. In the present study, elevated PlGF was observed in the infarcted brain after hMSC and PlGF-hMSC infusion, but PlGF levels were higher following infusion of the PlGF-hMSCs. PlGF induced angiogenesis and did not increase cerebral oedema as assayed by both *in vivo* MRI and histological analysis.

The therapeutic effect of PlGF-hMSC transplantation in the permanent rat MCAO model was observed even when applied 3 h after infarction. Thus, cellular delivery of PlGF by hMSCs or hypersecreting PlGF-hMSCs may have a therapeutic effect following cerebral ischaemia through neuroprotective and angiogenic mechanisms. These results do not rule out the potential beneficial effects of other trophic factors such as BDNF (Nomura *et al.*, 2005) that is secreted by hMSCs. BDNF hypersecreting hMSCs induced comparable beneficial effects as PlGF-hMSCs. It will be interesting to determine if there is enhanced recovery by simultaneous administration of both cell types.

Cell-based therapeutic approaches are being considered for a number of neurological diseases. Improved neurological function in experimental autoimmune encephalomyelitis (EAE) has been reported following intravenous infusion of hMSCs (Zhang *et al.*, 2005) and neurosphere-derived multipotent precursors (Pluchino *et al.*, 2003, 2005). Suggested mechanisms include reduction of inflammatory infiltration and demyelination, and elevation of trophic factors that may be neuroprotective or stimulate oligodendrogliosis. A cell-based therapy may have the advantage of exerting multiple therapeutic effects at various sites and times within the lesion, as the cells respond to a particular pathological microenvironment. As complex as these mechanisms are likely to be, our results indicate that PlGF contributes to neuroprotection and angiogenesis in cerebral ischaemia, and cellular delivery of PlGF to the brain can be achieved by intravenous delivery of hMSCs.

Acknowledgements

This work was supported in part by grants from the Japanese Ministry of Education, Science, Sports and Culture (16390414), Mitsui Sumitomo Insurance Welfare Foundation, JST (Japan, Science and Technology Corporation) Innovation Plaza Hokkaido Project, the National Multiple Sclerosis Society (USA) (RG2135; CA1009A10), the National Institutes of Health (NS43432), and the Medical and Rehabilitation and Development Research Services of the Department of Veterans Affairs.

References

Autiero M, Luttun A, Tjwa M, Carmeliet P. Placental growth factor and its receptor, vascular endothelial growth factor receptor-1: novel targets for stimulation of ischemic tissue revascularization and inhibition of angiogenic and inflammatory disorders. J Thromb Haemost 2003; 1: 1356–70.

Beck H, Acker T, Puschel AW, Fujisawa H, Carmeliet P, Plate KH. Cell type-specific expression of neuropilins in an MCA-occlusion model in mice suggests a potential role in post-ischemic brain remodeling. J Neuropathol Exp Neurol 2002; 61: 339–50.

Bederson JB, Pitts LH, Germano SM, Nishimura MC, Davis RL, Bartkowski HM. Evaluation of 2,3,5–triphenyltetrazolium chloride as a stain for detection and quantification of experimental cerebral infarction in rats. Stroke 1986; 17: 1304–8.

Carmeliet P, Moons L, Luttun A, Vincenti V, Compernolle V, De Mol M, et al. Synergism between vascular endothelial growth factor and placental growth factor contributes to angiogenesis and plasma extravasation in pathological conditions. Nat Med 2001; 7: 575–83.

Chen J, Li Y, Wang L, Lu M, Zhang X, Chopp M. Therapeutic benefit of intracerebral transplantation of bone marrow stromal cells after cerebral ischemia in rats. J Neurol Sci 2001a; 189: 49–57.

Chen J, Li Y, Wang L, Zhang Z, Lu D, Lu M, et al. Therapeutic benefit of intravenous administration of bone marrow stromal cells after cerebral ischemia in rats. Stroke 2001b; 32: 1005–11.

Chen X, Li Y, Wang L, Katakowski M, Zhang L, Chen J, et al. Ischemic rat brain extracts induce human marrow stromal cell growth factor production. Neuropathology 2002; 22: 275–9.

De Falco S, Gigante B, Persico MG. Structure and function of placental growth factor. Trends Cardiovasc Med 2002; 12: 241–6.

Dvorak HF, Dvorak AM, Manseau EJ, Wiberg L, Churchill WH. Fibrin gel investment associated with line 1 and line 10 solid tumor growth, angiogenesis, and fibroplasia in guinea pigs. Role of cellular immunity, myofibroblasts, microvascular damage, and infarction in line 1 tumor regression. J Natl Cancer Inst 1979; 62: 1459–72.

Hayashi T, Noshita N, Sugawara T, Chan PH. Temporal profile of angiogenesis and expression of related genes in the brain after ischemia. J Cereb Blood Flow Metab 2003; 23: 166–80.

Honma T, Honmou O, Iihoshi S, Harada K, Houkin K, Hamada H, et al. Intravenous infusion of immortalized human mesenchymal stem cells protects against injury in a cerebral ischemia model in adult rat. Exp Neurol 2006; 199: 56–66.

Iihoshi S, Honmou O, Houkin K, Hashi K, Kocsis JD. A therapeutic window for intravenous administration of autologous bone marrow after cerebral ischemia in adult rats. Brain Res 2004; 1007: 1–9.

Inoue M, Honmou O, Oka S, Houkin K, Hashi K, Kocsis JD. Comparative analysis of remyelinating potential of focal and intravenous administration of autologous bone marrow cells into the rat demyelinated spinal cord. Glia 2003; 44: 111–8.

Kinnaird T, Stabile E, Burnett MS, Shou M, Lee CW, Barr S, et al. Local delivery of marrow-derived stromal cells augments collateral perfusion through paracrine mechanisms. Circulation 2004; 109: 1543–9.

Kobune M, Kawano Y, Ito Y, Chiba H, Nakamura K, Tsuda H, et al. Telomerized human multipotent mesenchymal cells can differentiate into hematopoietic and cobblestone area-supporting cells. Exp Hematol 2003; 31: 715–22.

Kurozumi K, Nakamura K, Tamiya T, Kawano Y, Kobune M, Hirai S, et al. BDNF gene-modified mesenchymal stem cells promote functional recovery and reduce infarct size in the rat middle cerebral artery occlusion model. Mol Ther 2004; 9: 189–97.

Kurozumi K, Nakamura K, Tamiya T, Kawano Y, Ishii K, Kobune M, et al. Mesenchymal stem cells that produce neurotrophic factors reduce ischemic